PHYSICS

# Kinetic approach to superconductivity hidden behind a competing order

Hiroshi Oike[1,2]*, Manabu Kamitani[1], Yoshinori Tokura[1,2], Fumitaka Kagawa[1,2]*



**Exploration for superconductivity is one of the research frontiers in condensed matter physics. In strongly correlated electron systems, the emergence of superconductivity is often inhibited by the formation of a thermodynamically more stable magnetic/charge order. Thus, to develop the superconductivity as the thermodynamically most stable state, the free-energy balance between the superconductivity and the competing order has been controlled mainly by changing thermodynamic parameters, such as the physical/chemical pressure and carrier density. However, such a thermodynamic approach may not be the only way to materialize the superconductivity. We present a new kinetic approach to avoiding the competing order and thereby inducing persistent superconductivity. In the transition-metal dichalcogenide $IrTe_2$ as an example, by using current pulse–based rapid cooling of up to ~$10^7$ K $s^{-1}$, we successfully kinetically avoid a first-order phase transition to a competing charge order and uncover metastable superconductivity hidden behind. Because the electronic states at low temperatures depend on the history of thermal quenching, electric pulse applications enable nonvolatile and reversible switching of the metastable superconductivity, a unique advantage of the kinetic approach. Thus, our findings provide a new approach to developing and manipulating superconductivity beyond the framework of thermodynamics.**

## INTRODUCTION

Thermodynamics states that materials at equilibrium adopt the lowest free-energy state when several states are competing; this principle has provided solid and universal guidance in controlling static phases of matter. For instance, in alloys, one can materialize an intended structural form out of various candidate forms by tuning their composition, a control parameter of their free-energy balance (*1*). Similarly, in strongly correlated electron systems, the electrons' internal degrees of freedom can exhibit various ordered phases at low temperatures, and their free-energy balance is closely associated with electron bandwidth and band filling. Thus, pressure and/or carrier doping have been exclusively exploited when searching for superconductivity as the ground state (*2*–*4*). This approach is schematically illustrated in Fig. 1, which we call the thermodynamic approach.

Although the thermodynamic approach is literally based on thermodynamics and can hence be applied to a variety of systems, there is another phase-control method that is not properly described within the framework of thermodynamics, that is, the kinetic approach, a main subject in this report. The kinetic approach is based on the fact that within a considered time range, a system does not necessarily trace the global free-energy minimum and may be trapped in a local minimum, a metastable state. For instance, carbon steel changes its form upon cooling from face-centered cubic to body-centered cubic according to the temperature-dependent minimum free energy (*5*). However, this phase change is a first-order transition initiated by nucleation, and it can therefore be kinetically avoided when the system is sufficiently rapidly cooled to a certain low temperature. Such a kinetic approach based on thermal quenching has long been used in the fields of ferrous metallurgy and supercooled liquids to materialize higher-energy metastable structural forms, such as martensite (*6*) and glass (*7*, *8*); however, only recently has thermal quenching far beyond standard cooling rates come into use for controlling electronic/magnetic states in condensed matters (*9*–*12*). Here, we find that thermal quenching is capable of materializing persistent superconductivity that is otherwise superseded by a thermodynamically more stable magnetic/charge order. Such a kinetic approach enables nonvolatile and reversible switching of superconductivity with pulse application, providing a basis for superconducting devices that do not require band-filling control through gate electrodes or bandwidth control through piezo elements.

[1]RIKEN Center for Emergent Matter Science, Wako 351-0198, Japan. [2]Department of Applied Physics, The University of Tokyo, Tokyo 113-8656, Japan.
*Corresponding author. Email: oike@ap.t.u-tokyo.ac.jp (H.O.); kagawa@ap.t.u-tokyo.ac.jp (F.K.)

## RESULTS

### Material selection

For selecting a candidate material, we set the two criteria depicted in Fig. 1. First, the ground state is a magnetic/charge order, but a superconducting phase neighbors it with physical/chemical pressure or carrier doping as a control parameter. Second, the magnetic/charge order is formed through a first-order transition. We envisaged that in such a material, superconductivity would emerge as a metastable state if the formation of the more stable competing order is avoided kinetically under rapid cooling (see "Kinetic approach" in Fig. 1). Among many candidate materials, we targeted the transition-metal dichalcogenide $IrTe_2$, the phase diagram of which explicitly shows that a superconducting phase with $T_c^{onset} \approx 3.0$ to 3.1 K appears when a first-order charge-ordering transition is thermodynamically suppressed, in this case, by element substitution (Fig. 2A) (*13*–*15*). A recent scanning tunneling microscopy study on pristine $IrTe_2$ has shown that rapid cooling results in the emergence of superconducting patches at the surface (*16*); however, the signature of superconductivity has never been detected in macroscopic physical properties, indicating that the validity of our hypothetical kinetic approach toward macroscopic superconductivity still remains unclear.

### Thermal quenching

To this end, we focused on standard electric resistivity measurements and performed thermal quenching at an unconventionally high rate, >$10^6$ to $10^7$ K $s^{-1}$, from a sufficiently high temperature (≈300 to 400 K)

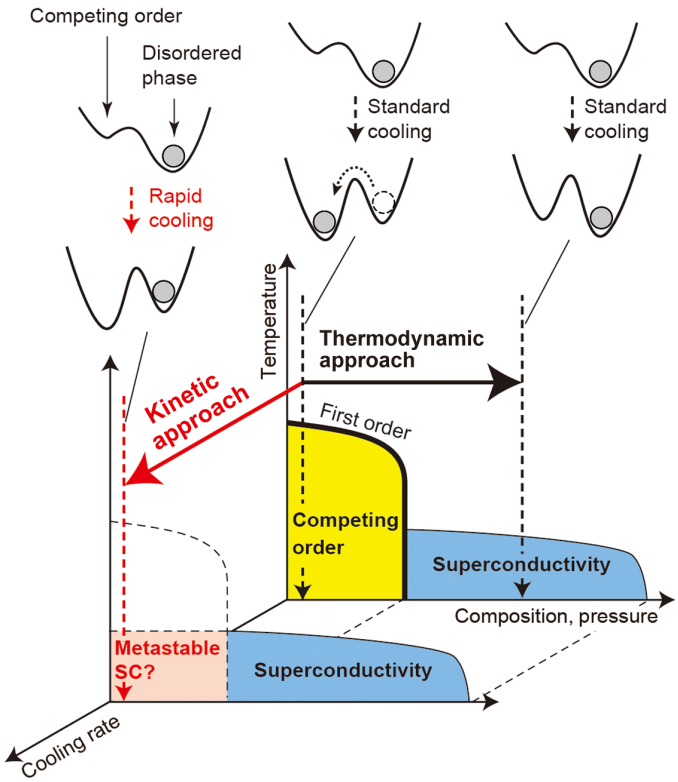


**Fig. 1. Scheme for thermodynamic and kinetic approaches to realizing superconductivity in certain strongly correlated electron systems.** The conceptual electronic phase diagram considered in this study is displayed with pressure/carrier doping as a control parameter. The double well and ball represent temperature-dependent schematic free-energy landscapes and realized electronic states in each cooling process, respectively. The thermodynamic approach, which can be advanced by increasing pressure or carrier doping, results in a change in the lowest free-energy state, from a certain competing order to a superconducting (SC) state. By contrast, the kinetic approach, which can be advanced by rapid cooling, allows the system to kinetically avoid the first-order phase transition to the competing order and thus to remain in a metastable supercooled state, which is expected to eventually turn into superconducting at low temperatures.

to 4 K. To achieve this quenching, we applied electric-pulse heating to a sample in contact with a substrate at 4 K (Fig. 2B), which is inevitably followed by rapid cooling after the pulse ends because of a substantial thermal gradient between the sample and the substrate (Fig. 2C) (see Materials and Methods and the Supplementary Materials). In implementing the kinetic approach based on thermal quenching, we also considered the sample volume $V$: Just as rapid cooling invariably results in a lower nucleation probability in terms of time, sample miniaturization makes nucleation less probable in terms of the number of nucleation sites contained in a specimen (*17*, *18*). Thus, sample miniaturization, in principle, can supplement the kinetic approach. Nevertheless, the sample volume is a "static" state variable and can also thermodynamically affect the free-energy balance through the change in the ratio between the bulk and surface energies. To exclusively highlight the kinetic aspect of the approach, we therefore focused on how the low-temperature electronic state varies when the quenching to 4 K is applied to $IrTe_2$ thin plates with different volumes.

The results are displayed in Fig. 2 (D to G). In a relatively large thin plate, #1 ($V \approx 130\ \mu m^3$), a sharp resistivity increase that signals the charge-order formation was observed at $T_{CO}^{cool} \approx 250$ K under slow cooling (Fig. 2D), and accordingly, the temperature-resistivity profile exhibited no signature of superconductivity at the lowest temperature (Fig. 2E). This behavior is in agreement with that of the bulk sample (*19*), and it can be regarded as a reference when the charge order is fully formed in a considered specimen. Notably, after performing quenching to 4 K at a cooling rate of $\sim 10^5$ K $s^{-1}$ by using the electric-pulse heating (figs. S1 to S3), a signature of superconductivity with $T_c^{onset} \approx 3.1$ K emerged (Fig. 2E), consistent with our working hypothesis. However, zero resistance was not reached, probably because of an insufficient superconducting volume fraction.

To achieve quenching-induced zero resistance with an experimentally accessible quenching rate, we next targeted a smaller sample: #2 ($V \approx 15\ \mu m^3$). As expected, a low-temperature resistivity profile resembling that of sample #1 postquenching was obtained without implementing quenching (Fig. 2G), consistent with the idea that sample miniaturization can supplement the kinetic approach, although a possible change in the free-energy balance cannot be ruled out. At higher temperatures, a broadened, relatively weak increase in resistivity was observed at $T_{CO}^{cool} \approx 200$ K (Fig. 2F), which was considerably lower than the case of sample #1. These observations suggest that the charge ordering was avoided in a certain fraction even under slow cooling, thus leading to superconductivity as a minor phase. We found that when the quenching ($\sim 10^7$ K $s^{-1}$) is applied, the quenched state exhibits a relatively sharp drop with $T_c^{onset} \approx 3.4$ K and reaches zero resistance (Fig. 2G). Similar behavior was also observed in another thin plate with a comparable volume, #3 ($V \approx 18\ \mu m^3$) (see fig. S4), thus establishing that zero resistance is achieved by quenching. The $T_c^{onset}$ of the emergent superconductivity in the quenched states is plotted in the phase diagram and found to be comparable to, or slightly higher than, those of doped $IrTe_2$ (Fig. 2A).

## Quenching-rate dependence

To gain further insight into how the applied quenching rate correlates with the emergence of the superconductivity, we tailored the quenching rate with ramp pulses (fig. S5) and systematically examined the low-temperature resistivity postquenching for thin plate #3. The results are summarized as a resistivity contour plot in Fig. 3. Here, two important aspects can be highlighted. First, as the rate of quenching to 4 K increases, the zero-resistance temperature $T_c^{zero}$ continuously increases, whereas $T_c^{onset}$ varies only weakly. Although the sample smallness makes it difficult to estimate the superconducting volume fraction via magnetic susceptibility measurements, this behavior can be understood by considering that the quenching rate continuously changes the superconducting volume fraction. Second, the systematic variations indicate that the quenched state hosting superconductivity is metastable. Moreover, the zero-resistance state is found to disappear if the quenched state is heated above 50 K and subsequently cooled (see fig. S6), consistent with the general propensity that a quenched state is metastable, and it reverts to a slowly cooled state if an annealing procedure is properly performed. Conversely, the metastability of the quenched state is practically robust below 50 K (greater than 1 week at 10 K), and thus, a magnetic field–induced superconducting-to-normal transition shows a reversible behavior (fig. S7).

## Nonvolatile switching

Finally, we show that the bistability consisting of the nonzero- and zero-resistance states, unveiled by the kinetic approach, raises an

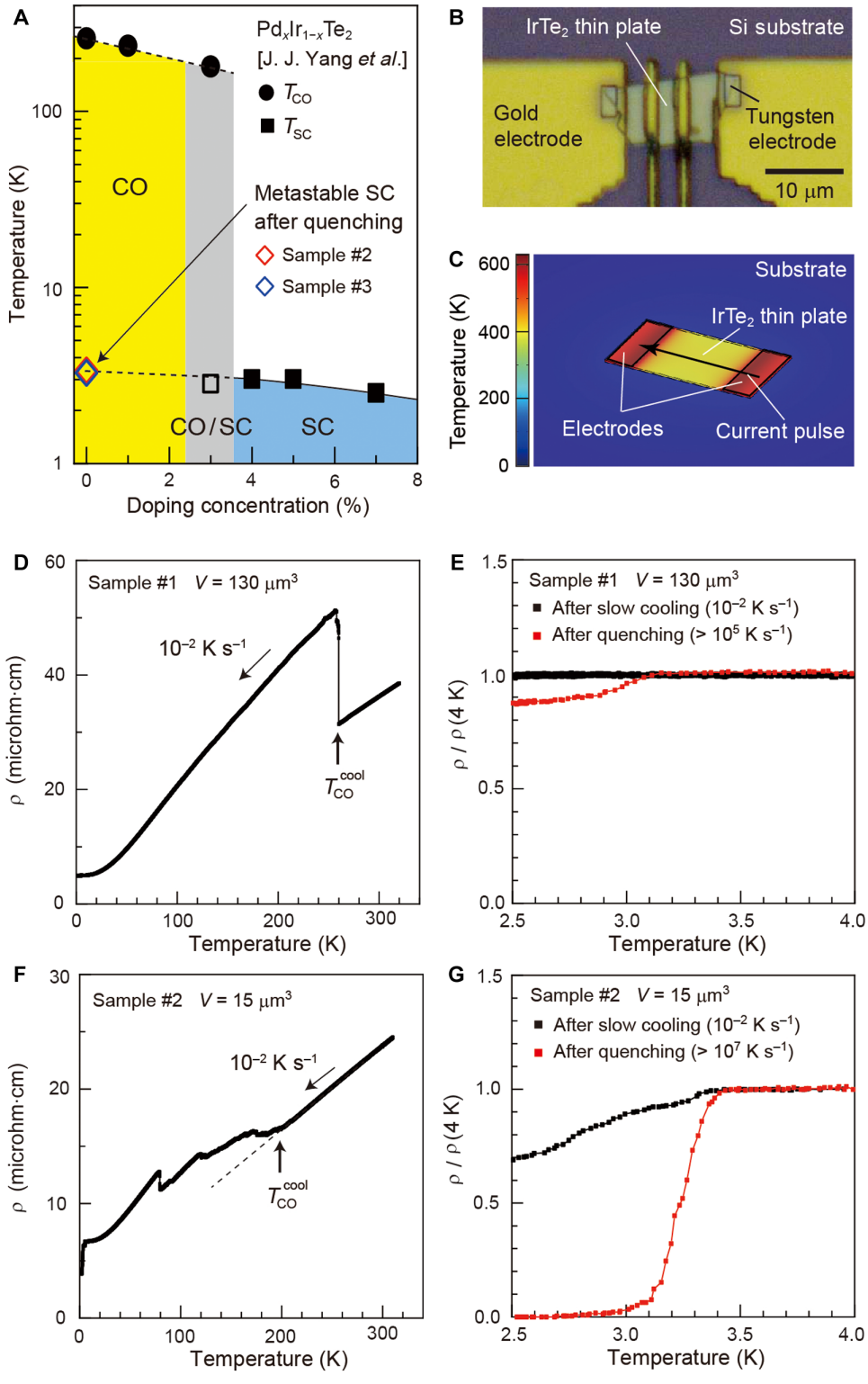


**Fig. 2. Demonstration of the kinetic approach to a superconducting state in nondoped $IrTe_2$.** (**A**) Electronic phase diagram of Pd-doped $IrTe_2$. CO and SC denote the charge-ordered and superconducting phases, respectively. The open diamonds represent the onset temperature of the emergent superconductivity in the quenched metastable state of nondoped $IrTe_2$ samples: #2 and #3. The data for the doped materials are taken from (*13*). (**B**) Photograph of a submicrometer-thick $IrTe_2$. (**C**) Schematic of the current pulse–based rapid-cooling method used in this study. At the end of an electric pulse, a large thermal gradient is realized between the sample and the substrate, thus enabling the rapid cooling of the sample after the pulse ends. The schematic is a result of our numerical simulation (see Materials and Methods and the Supplementary Materials). (**D** and **F**) Overall temperature-resistivity profiles of samples #1 (D) and #2 (F), the volumes of which are ≈130 and 15 μm$^3$, respectively. (**E** and **G**) Temperature-resistivity profiles of samples #1 (E) and #2 (G) near the superconductivity-onset temperature, which is measured after being slowly cooled and thermally quenched to 4 K.

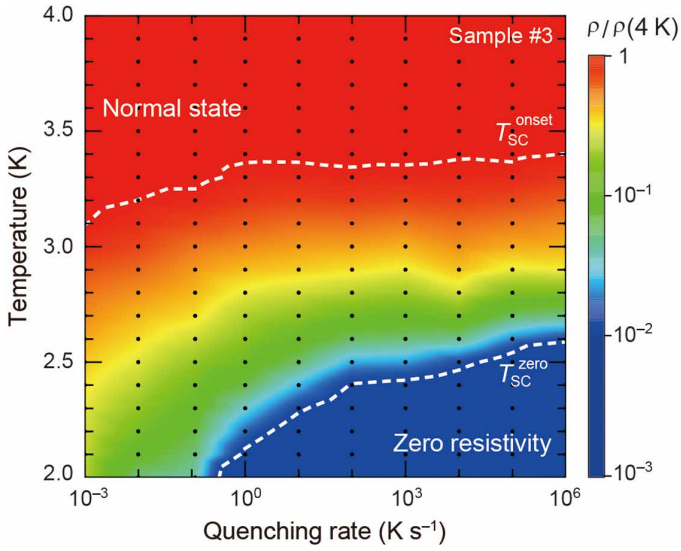


**Fig. 3. Contour plot of the electric resistivity postquenching to 4 K at various quenching rates in sample #3.** This figure represents an interplay between the quenching rate and the emergent superconductivity in nondoped $IrTe_2$. To clearly show the superconducting-transition onset, the data are normalized by the value at 4 K postquenching at each quenching rate.

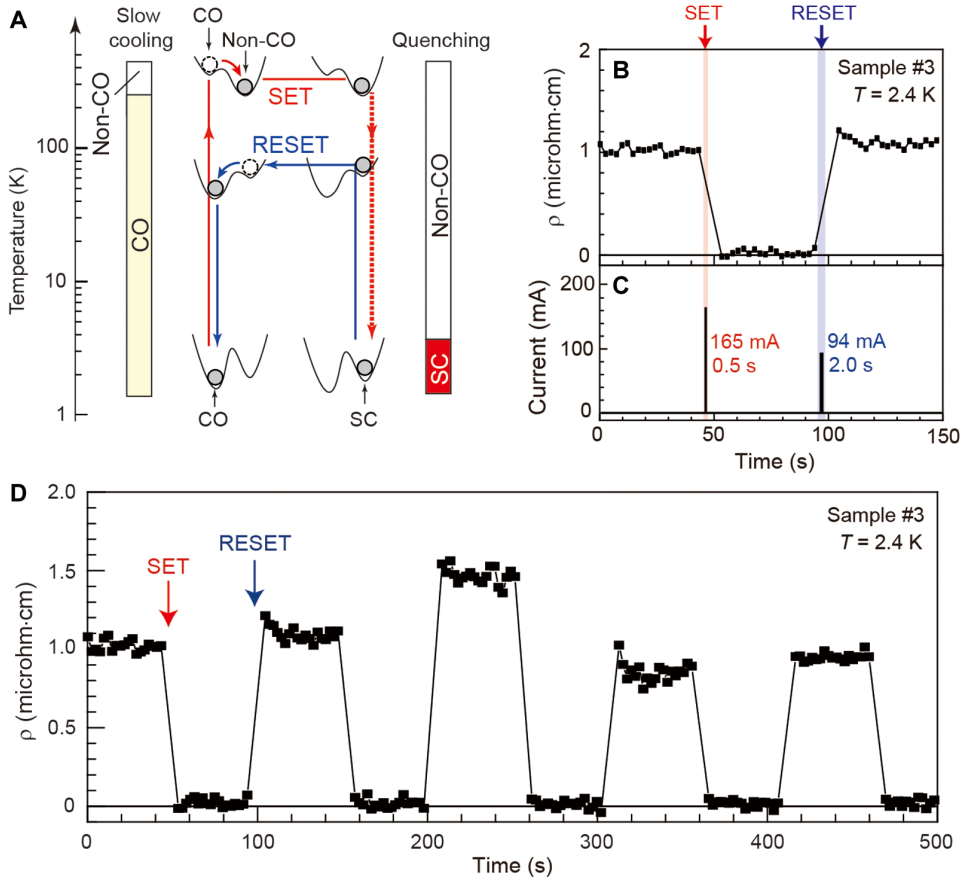


**Fig. 4. Nonvolatile superconducting phase change by the application of current pulses.** (**A**) Scheme for repeatable switching between the superconducting and charge-ordered states in terms of a schematic free-energy landscape and the kinetic approach. In the SET process, the application of a high-intensity current pulse results in the rapid cooling of the sample from a temperature above the charge ordering. In the RESET process, a pulse with moderate intensity and longer width is applied to heat the quenched state to a certain temperature below the charge ordering, facilitating relaxation to the charge order, which is more stable than the quenched metastable state. (**B** and **C**) Single-cycle operation of the nonvolatile switching. The time profiles of the resistivity and current are shown in (B) and (C), respectively. (**D**) Repetitive switching between the zero-resistance and nonzero-resistance states by the application of current pulses.

interesting possibility, that is, the design of a reversible superconducting switch based on applying electric pulses. The working principle considered here is illustrated in the schematic (Fig. 4A), and it is analogous to that of conventional phase-change memories (*20*, *21*), in which the operation is ultimately based on rapid temperature control using electric/optical pulses. In the forward switching from the nonzero-resistance slowly cooled to zero-resistance quenched states (the "SET" process), we used electric-pulse heating followed by rapid cooling at ~$10^7$ K $s^{-1}$ to a sample-holder temperature below $T_c^{zero}$. Similarly, the described annealing process of the quenched state can be substituted by the application of an electric pulse with relatively weak magnitude: During the pulse application (≈2 s), the quenched state is held at temperatures above 50 K, and after the pulse ends, the sample is promptly cooled (~$10^7$ K $s^{-1}$) to the sample-holder temperature, completing the backward switching (the "RESET" process).

The typical resistance-switching behavior is displayed in Fig. 4 (B and C). Current pulse–induced switching between zero- and nonzero-resistance states was successfully observed at 2.4 K in a nonvolatile manner without changing the sample-holder temperature. The switching is reproducible (Fig. 4D), thereby highlighting the deterministic nature of the working principle described (Fig. 4A). Such superconducting phase control with pulse application is a unique advantage of the kinetic approach implemented by thermal quenching. If the kinetic approach is implemented only by the sample miniaturization, then superconductivity invariably appears even under slow cooling (*22*), thus losing its controllability. Moreover, if one seeks to design a superconducting switching function within the framework of the thermodynamic approach, then the device would have to be equipped with certain elements that enable in situ and reversible control of pressure or carrier density at low temperatures (*23*–*25*).

## DISCUSSION

When the emergence of superconductivity is inhibited by a magnetic/charge order, it has widely been considered that, for the superconductivity to develop, the free-energy balance has to be modulated to make the superconducting state energetically most favored. To circumvent this thermodynamic constraint, highly nonequilibrium methods using intense light pulses have recently been exploited, and the superconductivity is actually induced out of a certain competing phase but only transiently (*26*). Our observations have shown that when the overall feature of a thermoequilibrium phase diagram agrees with that shown in Fig. 1, persistent superconductivity can be realized by another nonequilibrium method, that is, quenching the system to low temperatures such that nucleation of the competing order is no longer expected in the considered time range. Thus, our work provides some of the materials that have been categorized as nonsuperconducting with a fresh chance to yield metastable superconducting behavior.

## MATERIALS AND METHODS

### Sample preparation

Bulk single crystals of $IrTe_2$ were synthesized using the Te-flux method according to the literature (*19*). Submicrometer-thick crystals were exfoliated from a bulk single crystal with Scotch tape and transferred onto silicon (Si) or polyethylene naphthalate (PEN) substrates. Gold electrodes were prepared on the substrate and sample surface using photolithography methods. The electrodes on the sample surface were connected with those on the substrate by tungsten deposition using a focused-ion beam to ensure the electrical connection between them. An image of a typical sample is shown in Fig. 2B. The contact resistance depends on the area of the current electrode, and it is typically 1 to 3 ohms for each contact. The sample thickness was measured using scanning electron microscopy.

### Resistivity measurements

The resistivity under slow cooling was measured with the conventional four-probe method. A load resistor of 10 kilohms was connected in series with the sample. An AC voltage excitation of 333 Hz with a magnitude corresponding to 10 μA was generated at a lock-in amplifier (Signal Recovery, 7270) and applied to the circuit. Signals from the voltage probes were amplified with a low-noise preamplifier (NF Corporation, SA-410F3 or Stanford Research, SR560) and measured with the lock-in amplifier. The current flowing through the circuit was measured by probing the voltage drop at the load resistor with another lock-in amplifier.

### Pulse application

To feed a current pulse with a sufficient magnitude (160 and 19 mA for samples on Si and PEN substrates, respectively), a trapezoidal voltage that was generated using a function generator (NF Corporation, WF1947) was amplified using a high-speed bipolar power supply (NF Corporation, HSA4014). A load resistor of 2.5 ohms was connected in series with the sample and used to calculate the current flowing through the circuit. The time-varying voltages at the load resistor and the sample voltage-probes were amplified using a differential amplifier (NF Corporation, 5307) and a low-noise preamplifier (NF Corporation, SA-410F3 or Stanford Research, SR560), respectively, and the amplified voltages were monitored using a digitizer (National Instruments, NI PXIe-5122) or an analog input module (National Instruments, NI 9239). Thus, we obtained the time profiles of the current and sample resistivity during the pulse application. A switch system (Keithley 7001 equipped with 7011S) was used to switch the circuit between the resistivity-measurement and pulse-application setups.

## SUPPLEMENTARY MATERIALS

Supplementary material for this article is available at http://advances.sciencemag.org/cgi/content/full/4/10/eaau3489/DC1

Supplementary Materials and Methods

Fig. S1. Sample heating by a trapezoidal current-pulse application, followed by rapid cooling.

Fig. S2. Measurements of the highest quenching rate achieved in the present experiments.

Fig. S3. Simulation results of the quenching process for an $IrTe_2$ thin plate on Si and PEN substrates.

Fig. S4. Creation of persistent superconductivity by a current application in the $IrTe_2$ thin plate #3.

Fig. S5. Manipulation of the quenching rate by controlling the pulse fall time.

Fig. S6. Annealing process of the quenched metastable state in the $IrTe_2$ thin plate #3 on the Si substrate.

Fig. S7. Magnetic field effects on the emergent superconductivity in the quenched metastable states.

## REFERENCES AND NOTES

1. D. A. Porter, K. E. Easterling, M. Y. Sherif, *Phase Transformations in Metals and Alloys* (CRC Press, 2008).
2. E. Fradkin, S. A. Kivelson, J. M. Tranquada, *Colloquium*: Theory of intertwined orders in high temperature superconductors. *Rev. Mod. Phys.* **87**, 457–482 (2015).
3. E. Dagotto, *Colloquium*: The unexpected properties of alkali metal iron selenide superconductors. *Rev. Mod. Phys.* **85**, 849–867 (2013).

4. P. F. S. Rosa, J. Kang, Y. Luo, N. Wakeham, E. D. Bauer, F. Ronning, Z. Fisk, R. M. Fernandes, J. D. Thompson, Competing magnetic orders in the superconducting state of heavy-fermion $CeRhIn_5$. *Proc. Natl. Acad. Sci. U.S.A.* **114**, 5384–5388 (2017).
5. J. Chipman, Thermodynamics and phase diagram of the Fe-C system. *Metall. Mater. Trans. B.* **3**, 55–64 (1972).
6. D. S. Mackenzie, History of quenching. *Int. Heat Treat. Surf. Eng.* **2**, 68–73 (2013).
7. C. A. Angell, Formation of glasses from liquids and biopolymers. *Science* **267**, 1924–1995 (2011).
8. P. G. Debenedetti, F. H. Stillinger, Supercooled liquids and the glass transition. *Nature* **410**, 259–267 (2001).
9. H. Oike, F. Kagawa, N. Ogawa, A. Ueda, H. Mori, M. Kawasaki, Y. Tokura, Phase-change memory function of correlated electrons in organic conductors. *Phys. Rev. B* **91**, 041101 (2015).
10. H. Oike, A. Kikkawa, N. Kanazawa, Y. Taguchi, M. Kawasaki, Y. Tokura, F. Kagawa, Interplay between topological and thermodynamic stability in a metastable magnetic skyrmion lattice. *Nat. Phys.* **12**, 62–66 (2016).
11. G. Berruto, I. Madan, Y. Murooka, G. M. Vanacore, E. Pomarico, J. Rajeswari, R. Lamb, P. Huang, A. J. Kruchkov, Y. Togawa, T. LaGrange, D. McGrouther, H. M. Rønnow, F. Carbone, Laser-induced skyrmion writing and erasing in an ultrafast cryo-lorentz transmission electron microscope. *Phys. Rev. Lett.* **120**, 117201 (2018).
12. F. Kagawa, H. Oike, Quenching of charge and spin degrees of freedom in condensed matter. *Adv. Mater.* **29**, 1601979 (2017).
13. J. J. Yang, Y. J. Choi, Y. S. Oh, A. Hogan, Y. Horibe, K. Kim, B. I. Min, S.-W. Cheong, Charge-orbital density wave and superconductivity in the strong spin-orbit coupled $IrTe_2$:Pd. *Phys. Rev. Lett.* **108**, 116402 (2012).
14. S. Pyon, K. Kudo, M. Nohara, Superconductivity induced by bond breaking in the triangular lattice of $IrTe_2$. *J. Phys. Soc. Jpn.* **81**, 053701 (2012).
15. M. Kamitani, M. S. Bahramy, R. Arita, S. Seki, T. Arima, Y. Tokura, S. Ishiwata, Superconductivity in $Cu_xIrTe_2$ driven by interlayer hybridization. *Phys. Rev. B* **87**, 180501 (2013).
16. H. S. Kim, S. Kim, K. Kim, B. Il Min, Y.-H. Cho, L. Wang, S.-W. Cheong, H. Woong Yeom, Nanoscale superconducting honeycomb charge order in $IrTe_2$. *Nano Lett.* **16**, 4260–4265 (2016).
17. D. Turnbull, Kinetics of solidification of supercooled liquid mercury droplets. *J. Chem. Phys.* **20**, 411–424 (1952).
18. H. Oike, M. Suda, M. Kamitani, A. Ueda, H. Mori, Y. Tokura, H. M. Yamamoto, F. Kagawa, Size effects on supercooling phenomena in strongly correlated electron systems: $IrTe_2$ and θ-$(BEDT\text{-}TTF)_2RbZn(SCN)_4$. *Phys. Rev. B* **97**, 085102 (2018).
19. M. J. Eom, K. Kim, Y. J. Jo, J. J. Yang, E. S. Choi, B. I. Min, J.-H. Park, S.-W. Cheong, J. Sung Kim, Dimerization-induced fermi-surface reconstruction in $IrTe_2$. *Phys. Rev. Lett.* **113**, 266406 (2014).
20. M. Wuttig, N. Yamada, Phase-change materials for rewriteable data storage. *Nat. Mater.* **6**, 824–832 (2007).
21. S. Raoux, Phase change materials. *Annu. Rev. Mater. Res.* **39**, 25–48 (2009).
22. M. Yoshida, K. Kudo, M. Nohara, Y. Iwasa, Metastable superconductivity in two-dimensional $IrTe_2$ crystals. *Nano Lett.* **18**, 3113–3117 (2018).
23. A. D. Caviglia, S. Gariglio, N. Reyren, D. Jaccard, T. Schneider, M. Gabay, S. Thiel, G. Hammerl, J. Mannhart, J.-M. Triscone, Electric field control of the $LaAlO_3/SrTiO_3$ interface ground state. *Nature* **456**, 624–627 (2008).
24. M. Suda, Y. Kawasugi, T. Minari, K. Tsukagoshi, R. Kato, H. M. Yamamoto, Strain-tunable superconducting field-effect transistor with an organic strongly-correlated electron system. *Adv. Mater.* **26**, 3490–3495 (2014).
25. M. Suda, R. Kato, H. M. Yamamoto, Light-induced superconductivity using a photoactive electric double layer. *Science* **347**, 743–746 (2015).
26. D. Fausti, R. I. Tobey, N. Dean, S. Kaiser, A. Dienst, M. C. Hoffmann, S. Pyon, T. Takayama, H. Takagi, A. Cavalleri, Light-induced superconductivity in a stripe-ordered cupate. *Science* **331**, 189–191 (2011).


**Acknowledgments:** F.K. and H.O. thank Y. Kawasugi and R. Takagi for their valuable discussions. **Funding:** This work was partially supported by the Japan Society for the Promotion of Science KAKENHI (grant nos. 18K13512 and 18H01168). **Author contributions:** H.O. performed all the experiments and analyzed the data. M.K. grew the single crystals used for the study. F.K. and H.O. planned the project. H.O. and F.K. wrote the manuscript. H.O., F.K., and Y.T. discussed the results and commented on the manuscript. **Competing interests:** The authors declare that they have no competing interests. **Data and materials availability:** All data needed to evaluate the conclusions in the paper are present in the paper and/or the Supplementary Materials. Additional data related to this paper may be requested from the authors.

Submitted 1 June 2018
Accepted 31 August 2018
Published 5 October 2018
10.1126/sciadv.aau3489

**Citation:** H. Oike, M. Kamitani, Y. Tokura, F. Kagawa, Kinetic approach to superconductivity hidden behind a competing order. *Sci. Adv.* **4**, eaau3489 (2018).